

# Emissivity and catalycity measurements on SiC-coated carbon fibre reinforced silicon carbide composite

Davide Alfano<sup>a,\*</sup>, Luigi Scatteia<sup>a</sup>, Stefania Cantoni<sup>a</sup>, Marianne Balat-Pichelin<sup>b</sup>

<sup>a</sup> CIRA-Centro Italiano Ricerche Aerospaziali, 81043 Capua (CE), Italy

<sup>b</sup> PROMES-CNRS Laboratory, 7 rue du four solaire, 66120 Font-Romeu Odeillo, France

Received 15 April 2008; received in revised form 2 December 2008; accepted 5 December 2008

Available online 10 January 2009

## Abstract

The emissivity and the catalytic efficiency related to atomic oxygen recombination were experimentally investigated in the range 600–1600 °C for a carbon fibre reinforced silicon carbide composite produced by polymer vapour infiltration and then coated with SiC by chemical vapour deposition. High emissivity (about 0.7 at 1600 °C) and low recombination coefficients (on average 0.07 at 1500 °C) were found for all the samples tested. The experimental data showed a marked effect of the surface finish on the catalytic behaviour only: C/SiC samples belonging to the same production batch but having slightly different surface morphology, while exhibiting the same catalycity trend, are characterized by detectable differences in absolute values of the recombination coefficient. Micro-structural investigations performed on post-test samples have shown the formation of a silica-based glassy layer and have confirmed that the oxidation of C/SiC lies on the boundary line between the active and passive mechanism.

© 2008 Elsevier Ltd. All rights reserved.

**Keywords:** B. Composites; C. Chemical properties; C. Optical properties; D. Carbon/SiC; Thermal protection system

## 1. Introduction

Carbon fibre reinforced silicon carbide composite (C/SiC) is a ceramic matrix composite characterized by good mechanical properties, thermo-mechanical stability and fracture toughness: being a long-fibre reinforced composite, its fracture behaviour sets it apart from conventional monolithic ceramics, allowing for a variety of uses in which damage tolerance, low density, and high fracture toughness at high temperatures are the main requirements. One of the most relevant application fields of C/SiC lies within the aerospace sector and concerns the manufacturing of structural thermal protection systems (TPSs) for re-entry vehicles, where good thermo-mechanical properties at high temperature associated with oxidation resistance are required.<sup>1–9</sup>

The good resistance to oxidation processes at high temperatures, both in static and dynamic oxidizing environmental, is indeed another core characteristic of C/SiC as opposed to other structural ceramic matrix composites (CMCs) like the carbon/carbon (C/C). This important property is guaranteed by the

passivating effect of silica (SiO<sub>2</sub>) formed by passive oxidation of the SiC matrix. When SiC undergoes passive oxidation<sup>10–15</sup> SiC and the carbon fibres are protected by formation of stable silica-based glassy layers (SiO<sub>2</sub>) which provide an effective barrier to the oxygen diffusion.<sup>16–20</sup> In order to improve further the oxidation resistance of C/SiC, protective coatings<sup>19–24</sup> usually based upon SiC, and applied by chemical vapour deposition (CVD), can be employed and that is the case in most space applications, where high reliability is usually a mandatory requirement.

While SiC-coated C/SiC composites have been studied for quite a long time in the space field, and have been fully characterized in their base thermo-mechanical properties, little or no data at all is available to date on their radiative and surface catalytic behaviour at high temperature. Nonetheless, emissivity and surface catalycity represent key parameters for space re-entry thermal protection system applications. Since Earth re-entry phase takes place in low pressures<sup>25–30</sup> the radiation becomes the main method to dissipate heat in order to reduce the surface temperature. Moreover, when crossing the atmosphere, a space vehicle creates a shock wave leading to very high temperatures. The excited species (atoms, ions, molecules, electrons) created in this phase diffuse in the boundary layer and react with the materials of the vehicle with the final effect to degrade them. The surface of the spacecraft could also act

\* Corresponding author. Fax: +39 0823 623 515.  
E-mail address: [d.alfano@cira.it](mailto:d.alfano@cira.it) (D. Alfano).

as a “catalyst” for recombination processes of atomic species (nitrogen and specially oxygen) to form molecular ones ( $O_2$ ,  $N_2$ , and  $NO$ ). Since recombination processes are exothermic (498 kJ released per mole of  $O_2$  formed, 945 kJ per mole of  $N_2$ , and 415 kJ per mole of  $NO$ ),<sup>31,32</sup> part of the released energy is transferred to the surface of TPSs with the consequent increasing of their temperature.<sup>33–37</sup>

Therefore, high emissivity (above 0.7) and low surface catalycity (recombination coefficient's values below 0.1) greatly improve the material performance in re-entry conditions, by reducing temperature gradients and thermal stresses in the structure, thus enabling the re-entry vehicle to operate under higher heat flux conditions. A reliable experimental evaluation of these parameters is required to feed aero-convective heating computations that, in absence of experimental data, have to rely on extremely conservative theoretical values.

In this paper, the results of an in-depth experimental investigation into the efficiency of a SiC-coated C/SiC CMC for heat radiation and for the recombination of atomic oxygen are reported. The study is focused on a high temperature regime (from 600 to 1600 °C) that was achieved using the solar furnaces, associated facilities *Moyen d'Essai et de Diagnostic en Ambiance Spatiale Extrême* (MEDIASE) and *Moyen d'Essai Solaire d'Oxydation* (MESOX) and measurement methods available at PROMES-CNRS laboratory in France. Total hemispherical emissivity and recombination coefficient for atomic oxygen were characterized in the range 600–1600 °C. Supportive micro-structural analyses based upon XRD and SEM were carried out in order to correlate the obtained results to the surface modifications occurring in the material during high temperature exposure. The C/SiC tested is produced by MT-Aerospace and specifically designed for TPS applications.<sup>28,38–40</sup>

## 2. Material and experimental procedures

### 2.1. Material

The material tested is a SiC-coated two-dimensional C/SiC ceramic matrix composite, produced by MT-Aerospace and marketed under the name Keraman®. The C/SiC is produced by polymer vapour infiltration (PVI) using carbon fibres with filament diameter of 7  $\mu\text{m}$ . The SiC coating is applied by CVD and is characterized by an average thickness of 60–80  $\mu\text{m}$ .

### 2.2. Emissivity measurement method

Total hemispherical emissivity  $\varepsilon^{\wedge}(T)$  as a function of temperature  $T$  has been measured in the range 700–1600 °C using a direct method<sup>41</sup> with the MEDIASE set-up developed at PROMES-CNRS laboratory<sup>42–44</sup> under the Solar Facilities for Europe (SOLFACE) program (6th Framework Program—European Community). Although the temperature values reached by different parts of a TPS during the re-entry phase in Earth's atmosphere depends on the geometry of the spacecraft and on the specific re-entry trajectory, the chosen temperature range (700–1600 °C) to perform emissivity and catalycity measurements is relevant to describe the typical re-

entry conditions of a blunt-body winged re-entry vehicle (e.g. the Space Shuttle or the X-38 vehicle).<sup>25,45,46</sup>

In our experiments the specimen, characterized by a diameter of 40 mm and by a thickness equal to 2 mm, was heated by concentrated solar energy at the focus of the 1 MW solar furnace. On the back face of the sample, total (wavelength range 0.6–40  $\mu\text{m}$ ) and spectral (wavelength 5  $\mu\text{m}$ ) directional (0–80° by 10° step) radiance were measured by mean of a moving three-mirrors goniometer that collects the radiation emitted from the sample at different angles. The total directional radiance was measured with a radiometer calibrated against a reference blackbody. Each emissivity experiment has been carried out in air at 4 and 200 Pa obtaining the total hemispherical emissivity values by integration of directional emissivity ones. Every hemispherical emissivity value is characterized by accuracy of  $\pm 5\%$ .

Further details about the facilities used to measure directional emissivity and the method to obtain hemispherical emissivity values starting from the directional radiance ones are widely described elsewhere.<sup>41–44</sup>

### 2.3. Catalycity measurement method

The catalytic efficiency of the material for the recombination of atomic oxygen was studied by means of a direct method for the measurement of the recombination coefficient  $\gamma_o$ , defined as the ratio of the flux of atomic oxygen that recombines on the surface to that of the total atomic oxygen impinging the surface of the sample.

The atomic oxygen recombination coefficient  $\gamma_o$  was determined by measuring the concentration gradient of atomic oxygen in proximity of the sample surface by means of actinometry and optical emission spectroscopy (OES) techniques. In any case more and wide information about the method and the facilities used to evaluate the  $\gamma_o$  coefficient are reported in Refs. 47–49. In order to use the monochromatic optical pyrometer to measure the sample temperature during catalycity experiments, the normal spectral (5  $\mu\text{m}$ ) emissivity was recorded during the emissivity tests. On the basis of these results, a constant normal emissivity of 0.90 at 5  $\mu\text{m}$  was chosen for each tested sample. All tests have been carried out in MESOX set-up (developed at PROMES-CNRS) on discs 25 mm in diameter and 2 mm thickness in the range of temperature 500–1530 °C, and at total air pressure of 200 Pa. The concentration of atomic oxygen in the conditions of the measurements is about  $10^{22}$  atoms  $\text{m}^{-3}$  and the degree of dissociation is 80%.<sup>50</sup> Each recombination coefficient is characterized by an accuracy of  $\pm 30\%$ .

### 2.4. Micro-structure characterization methods

The sections of all specimens were examined by scanning electron microscopy (SEM) using a Oxford Instrument Leica S440. Samples for SEM observations were prepared using argon plasma sputtering with gold electrode to obtain a sample covered with a 50 Å gold layer. The measurements were performed in high vacuum ( $10^{-4}$  Pa). The cross-sections were obtained by cutting the discs along their diameter using a HER-

Table 1  
Values of total hemispherical emissivity measured at 4 and 200 Pa on CVD SiC-coated C/SiC.

Total pressure (Pa)	Temperature (°C)	Total hemispherical emissivity ( $\epsilon^{\text{h}}$ ) (0.6–40 $\mu\text{m}$ )
200	746 $\pm$ 8	0.57 $\pm$ 0.03
	947 $\pm$ 10	0.71 $\pm$ 0.04
	1118 $\pm$ 12	0.73 $\pm$ 0.04
	1354 $\pm$ 14	0.73 $\pm$ 0.04
	1422 $\pm$ 15	0.72 $\pm$ 0.04
	1624 $\pm$ 17	0.74 $\pm$ 0.04
4	841 $\pm$ 8	0.59 $\pm$ 0.03
	947 $\pm$ 10	0.69 $\pm$ 0.03
	1144 $\pm$ 12	0.71 $\pm$ 0.04
	1347 $\pm$ 14	0.72 $\pm$ 0.04
	1441 $\pm$ 15	0.70 $\pm$ 0.03

GON MT60 diamond cutting machine tool with diamond wheel 1.2 cm thick.

X-ray diffraction (XRD) investigations were performed on samples tested with MEDIASE and MESOX facilities. X-ray diffraction patterns ( $2\theta = 10\text{--}60^\circ$ ) were obtained with nickel-filtered  $\text{CuK}\alpha$  radiation with an automatic Bruker diffractometer.

### 3. Experimental results

#### 3.1. Emissivity measurements

Total hemispherical emissivity values measured at 4 and 200 Pa are listed in Table 1 and plotted in Fig. 1. In the examined temperature range, there is no significant difference between the emissivity values measured at 4 and at 200 Pa (the observed differences lie in the experimental uncertainty). In both cases the emissivity values show a similar trend increasing from  $\sim 0.6$  to  $\sim 0.7$  in the temperature range 750–1000 °C then staying almost constant in the temperature range 1000–1600 °C with an average value of about 0.7. The sample tested in the MEDIASE set-up exhibits the formation on its surface of a protective scale of silica detected by X-ray diffraction analyses (Fig. 2). In the XRD pattern shown in Fig. 2, the peak of  $\beta\text{-SiC}$  at  $35.8^\circ$  and the peak at  $26.2^\circ$  related to the reflection [1 0 1] of quartz are evident.

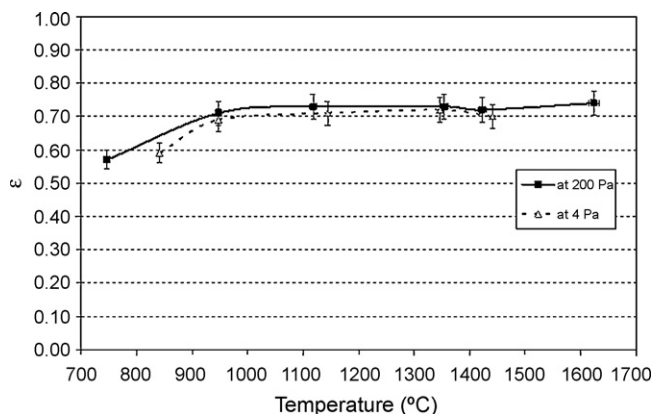


Fig. 1. Total hemispherical emissivity values of CVD SiC-coated C/SiC samples measured at 4 Pa (triangles) and at 200 Pa (squares).

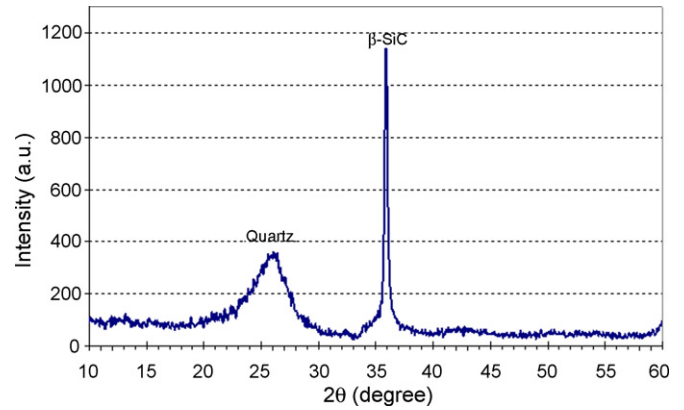


Fig. 2. X-ray diffraction patterns of the CVD SiC-coated C/SiC sample after the emissivity measurement performed with the MEDIASE facility.

This protective layer is not thermodynamically stable: actually, the partial pressures of both gaseous  $\text{SiO}_2$  and  $\text{SiO}$  are not negligible and indeed comparable in these experimental conditions. In fact, as theoretically demonstrated by means of the volatility diagrams of  $\beta\text{-SiC}$  reported in Ref. 10, at 1500 °C and at total air pressure of 200 Pa silicon carbide exhibits active oxidation. This result is confirmed by experimental data obtained by tests performed under standard air on C/SiC composites with a coating of  $\beta\text{-SiC}$  deposited by chemical vapour deposition: at 200 Pa the threshold temperature for the transition passive/active oxidation of CVDed samples is 1600–1700 °C.<sup>14,15</sup>

Considering the experimental conditions reached during the emissivity experiments, the oxidation process of the SiC coating falls on the boundary line between active and passive oxidation with the consequential ablation of the sample surface due to the loss of silicon as  $\text{SiO}_2$  and  $\text{SiO}$ . The degradation of the sample surface is evident by comparing the optical pictures of two samples heated up to 1600 °C at 4 and 200 Pa to the picture of the pristine one (Fig. 3). The quite strong evaporation–condensation of  $\text{SiO}_2$  is also confirmed by the appearance after the test of a thin layer of white powder on the surface of the sample holder of the MEDIASE set-up (Fig. 4) probably due to the condensation process of silica vapours on the cold surface of the sample holder (Fig. 4b). The surface ablation becomes more evident when at 1500 °C the pressure decreases at 4 Pa (Fig. 3c) because the partial pressure of  $\text{SiO}$  becomes slightly higher than that of  $\text{SiO}_2$ . In these experimental conditions the complete transition from passive behaviour to active oxidation occurs.<sup>13–15</sup>

Cross-section SEM images of the pristine and tested sample are compared in Fig. 5: after oxidation at 1600 °C the sample continues to show a relatively compact coating with the thickness of about 40–50  $\mu\text{m}$  which, however, is formed by unoxidized SiC and glass silica as demonstrated by the X-ray diffraction pattern carried out after the emissivity test and shown in Fig. 2.

The average hemispherical emissivity value of about 0.7 measured in the temperature range 1000–1600 °C is in line with data retrieved on silica-covered surfaces on different ceramic materials,<sup>51,52</sup> confirming that the radiative behaviour of the SiC-coated C/SiCs is mainly dictated by the surface glassy oxide scale.



Fig. 3. Pictures of the emitting surface of the sample CVD SiC-coated C/SiC (a) before and (b) and (c) after the emissivity experiment carried out increasing the temperature from 600 °C up to about 1600 °C at air pressure of 200 and 4 Pa, respectively.

### 3.2. Catalycity measurements

Two identical C/SiC specimens (labelled as A and B) were tested in MESOX facilities in order to measure the recombination coefficient for atomic oxygen ( $\gamma_o$ ). In Fig. 6 the logarithm of  $\gamma_o$  for the two samples respect the reciprocal of the absolute temperature is plotted in accordance with the well-known Arrhenius equation<sup>53</sup>:

$$\gamma_o = A \exp\left(\frac{-E_a}{RT}\right) \quad (1)$$

where  $A$  is the pre-exponential coefficient,  $E_a$  the activation energy of the oxygen recombination process,  $R$  the universal gas constant, and  $T$  is the absolute temperature.

Both samples conform approximately to the Arrhenius law that predicts a linear behaviour in the examined temperature range. The Arrhenius parameters ( $A$  and  $E_a$ ) used to fit by Eq. (1) and the values of  $\gamma_o$  measured at the maximum temperature reached during the tests are summarized in Table 2. The values of  $\gamma_o$  coefficients exponentially increase with the temperature starting from about 0.001 at 527 °C to about 0.07 at 1527 °C. Differences between the values of  $\gamma_o$  coefficients for

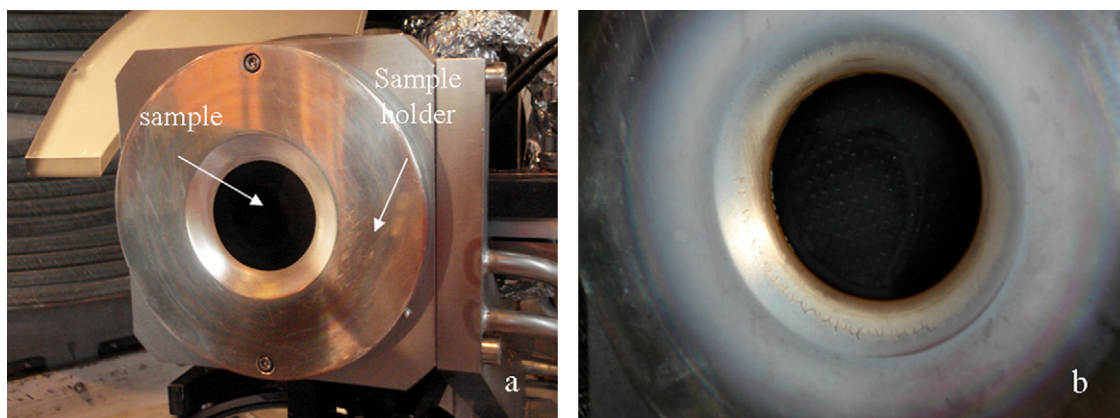


Fig. 4. (a) Sample of CVD SiC-coated C/SiC in the sample holder of the MEDIASE facility before testing and (b) detail of the sample holder after the emissivity measurement.

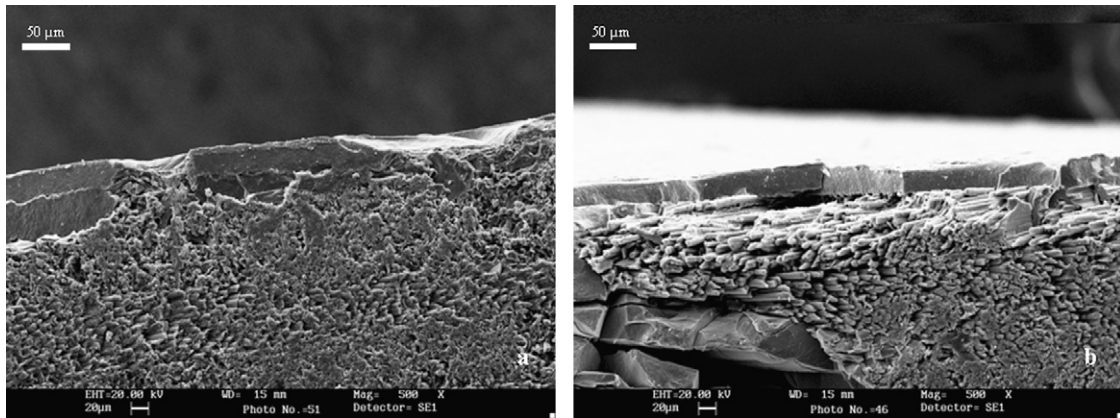


Fig. 5. Cross-section SEM micrographs of (a) pristine sample and (b) after emissivity measurement performed at about 1600 °C and 200 Pa.

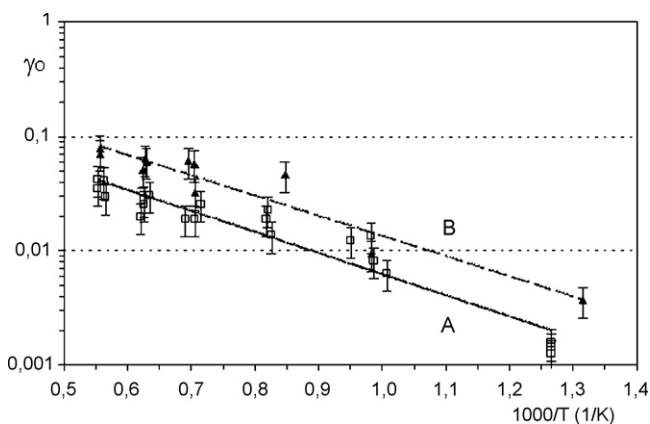


Fig. 6. Evolution of the recombination coefficient for atomic oxygen versus reciprocal absolute temperature for the two CVD SiC-coated C/SiC samples A and B. Both the measurements were performed at 200 Pa of total air pressure.

the two sets of measurements are evident with particular reference to low temperatures. This behaviour could be explained considering that each sample tested has a different surface roughness which strongly depends on the manufacturing process. For example, in Fig. 7 the pictures of the two samples manufactured by PVI and employed to perform emissivity tests are shown: the different roughness structure of the two samples is evident by the simple macroscopic and optical examination. In any case the comparable values of the slope of the fitting curves should seem to confirm the reproducibility of the catalytic experiments by means of them the activation energy for the atomic oxygen recombination process of C/SiC has been estimated equal to about 35 kJ/mol.

In Fig. 8 the cross-section SEM images of the samples A and B after catalytic test are displayed. The surface of the specimens are characterized by a compact and uniform layer with

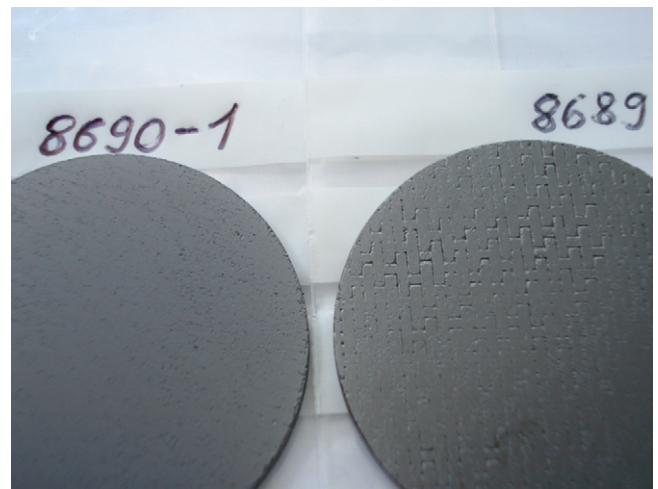


Fig. 7. Pictures of the surface of two CVD SiC-coated C/SiC specimens obtained by physical vapour infiltration and employed to perform emissivity tests with the MEDIASE facility.

thickness of 25–35 μm that is slightly thinner than the SiC coating of the pristine sample (Fig. 5a). This layer is formed by not oxidized SiC mixed with a glass silica layer as confirmed by X-ray diffraction patterns which were performed on the samples A and B and are not shown here because are equivalent to the pattern displayed in Fig. 2. In any case the experimental catalytic conditions activate on the two samples A and B the net weight loss that has never been more than 0.6 wt%. The experimental conditions applied during the catalytic measurements lie on the boundary line between the active and passive oxidation process.<sup>14,15</sup> Then the plasma flux activates the passive oxidation process of the C/SiC samples associated with the formation of a silica glassy oxide scale, and, at the same time, the

Table 2

Parameters of the Arrhenius type expression (Eq. (1)) used to fit the measured recombination coefficients ( $\gamma_0$ ) plotted on Fig. 2, and mean measured values of  $\gamma_0$  at 1527 °C related to the two tested samples of CVD SiC-coated C/SiC.

Sample	Pre-exponential coefficient (A)	$E_a/R$ (K)	Correlation coefficient	Activation energy (kJ/mol)	Mean $\gamma_0$ measured at 1527 °C
A	0.436	4.251	0.913	35.3	0.0368
B	0.792	4.075	0.907	33.9	0.0744

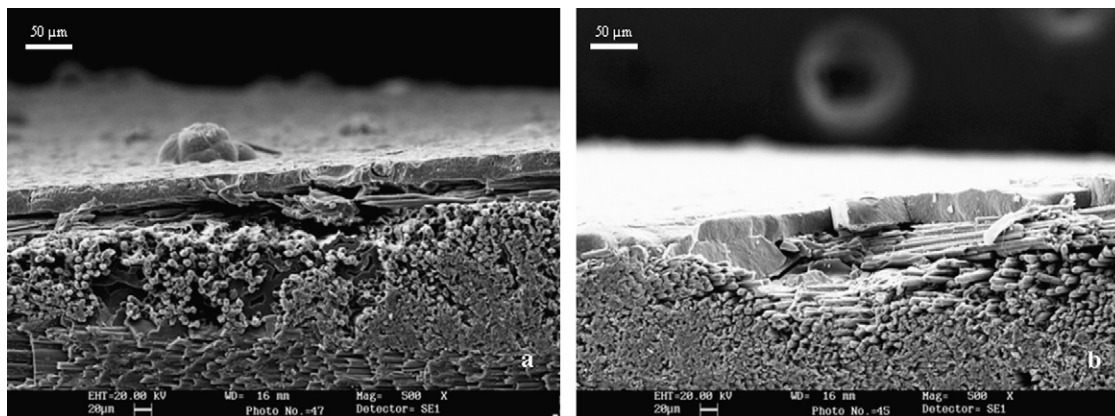


Fig. 8. Cross-section SEM micrographs of the sample (a) A and (b) B after the catalycity test performed at 200 Pa.

partial ablation of the samples that is due to the loss of silicon as  $\text{SiO}_2$  and  $\text{SiO}$ . Coherently with the micro-structural results, at higher temperature (about  $1500^\circ\text{C}$ ) the values of  $\gamma_o$  reported in this work are comparable to recombination coefficients for oxygen atoms measured for  $\beta$ -cristobalite.<sup>47,48</sup>

#### 4. Conclusions

In this paper the total hemispherical emissivity and the recombination coefficient of atomic oxygen on the surface of SiC-coated C/SiC composite are presented. The emissivity tests, conducted using the MEDIASE facility, have highlighted that across the temperature range  $600$ – $1600^\circ\text{C}$  and both at 4 than 200 Pa the material displays a high emissivity with an average value of about 0.7. This value is in line with data retrieved on silica-covered surfaces on different ceramic materials, confirming that the radiative behaviour of the SiC-coated C/SiCs is mainly dictated by the surface glassy oxide scale.

The catalycity evaluation performed using the MESOX facility have on the other hand shown a low oxygen recombination coefficient at high temperature (about 0.07 at  $1500^\circ\text{C}$ ). Tests performed on two samples have also shown the strong dependence of the recombination coefficient on the surface morphology, which may slightly vary from sample to sample due to manufacturing issues: samples of the same production batch have indeed shown different values of the recombination coefficient while having the same overall catalycity trend. In any case the results obtained allow the use in computations of a recombination coefficient value of 0.1 for temperature up to  $1500^\circ\text{C}$  (as a good compromise between the fully catalytic case with  $\gamma = 1$  and the maximum measured value of about 0.07). The low catalycity exhibited by the investigated C/SiC further confirms its suitability for the intended application in the manufacturing of hot structures for re-entry vehicles.

Micro-structural investigations conducted on the tested samples have allowed to confirm that the oxidation of C/SiC lies on the boundary line between the active and passive mechanism at the higher temperature level correlated to the formation of a silica-based glassy layer and the contemporaneous little mass loss.

#### Acknowledgments

This study was realized through the SOLFACE-FP6 program, project “Sharp Hot Structures”, contract no. RITA CT-2003-507091 and the authors thank J.L. Sans from PROMES-CNRS laboratory for the emissivity measurements and M. Passarelli for the catalycity tests. The authors also wish to thank Dr. Karin E. Handrick from MT-Aerospace AG for the C/SiC samples.

#### References

1. Naslain, R., *High Temperature Ceramic Matrix Composites*. Woodhead Publications, Bordeaux, 1993, pp. 215–229.
2. Laux, T., Ullmann, T., Auweter-Kurtz, M., Hald, H. and Kurz, A., Investigation of thermal protection materials along an X-38 re-entry trajectory by plasma wind tunnel simulations. In *Proceeding of the 2nd International Symposium on Atmospheric Reentry Vehicles and Systems*, 2001, pp. 1–9.
3. Naslain, R., Lamalle, J. and Zulian, J. L., Composite materials for high temperature applications. In *Proceedings of the AMAC*, 1990, pp. 315–325.
4. Messiah, A., *Developments in the Science and Technology of Composite Materials*. Elsevier, London, 1989, pp. 99–110.
5. Chawla, N., Holmes, J. W. and Lowden, R. A., The role of interfacial coatings on the high frequency fatigue behavior of Nicalon/C/SiC composites. *Scr. Mater.*, 1996, **35**, 1411–1416.
6. Lamouroux, F., Bourrat, X., Sevely, J. and Naslain, R., Structure/oxidation behaviour relationship in the carbonaceous constituents of 2D-C/PyC/SiC composites. *Carbon*, 1993, **31**, 1273–1288.
7. Torben, K. J. and Povl, B., Mechanical properties of two plain-woven chemical vapor infiltrated silicon carbide-matrix composites. *J. Am. Ceram. Soc.*, 2001, **84**, 1043–1051.
8. Mühlratzer, A. and Leuchs, M., Applications of non-oxide CMCs. In *Proceedings of the 4th International Conference on High Temperature Ceramic Matrix Composites*, 2001, pp. 288–298.
9. Harnisch, B., Kunkel, B., Deyerler, M., Bauereisen, S. and Papenburg, U., Ultra-lightweight C/SiC mirrors and structures. *ESA Bull.*, 1998, **95**, 4–8.
10. Heuer, A. H. and Lou, V. L. K., Volatility diagrams for silica, silicon nitride, and silicon carbide and their application to high temperature decomposition and oxidation. *J. Am. Ceram. Soc.*, 1990, **73**, 2785–3128.
11. Schneider, B., Guette, A., Naslain, R., Cataldi, M. and Costecalde, A., A theoretical and experimental approach to the active-to-passive transition in the oxidation of silicon carbide. *J. Mater. Sci.*, 1998, **33**, 535–547.
12. Jacobson, N. S., Corrosion of silicon-based ceramics in combustion environments. *J. Am. Ceram. Soc.*, 1993, **76**, 3–28.
13. Fahrenoltz, W. G., Thermodynamic analysis of  $\text{ZrB}_2$ -SiC oxidation: formation of a SiC-depleted region. *J. Am. Ceram. Soc.*, 2006, **90**, 143–148.

14. Balat, M. J. H., Determination of the active-to-passive transition in the oxidation of silicon carbide in standard and microwave-excited air. *J. Eur. Ceram. Soc.*, 1996, **16**, 55–62.
15. Morino, Y., Yoshinaka, T., Auweter-Kurtz, M., Hilfer, G., Speckmann, H.-D. and Sakai, A., Erosion characteristics of SiC coated C/C materials in arc heated high enthalpy air flow. *Acta Astro.*, 2002, **50**, 149–158.
16. Opeka, M. M., Talmy, I. G. and Zaykoski, J. A., Oxidation-based materials selection for 2000 °C + hypersonic aerosurfaces: theoretical considerations and historical experience. *J. Mater. Sci.*, 2004, **39**, 5887–5904.
17. Rezaie, A., Fahrenholtz, W. G. and Hilmis, G. E., Evolution of structure during the oxidation of zirconium diboride–silicon carbide in air up to 1500 °C. *J. Eur. Ceram. Soc.*, 2007, **27**, 2495–2501.
18. Damjanović, T., Argiris, C., Jokanović, B., Borchardt, G., Moritz, K., Müller, E. et al., Oxidation protection of C/C–SiC composites by an electrophoretically deposited mullite precursor: cyclic thermogravimetric analysis. *J. Eur. Ceram. Soc.*, 2007, **27**, 1299–1302.
19. Cheng, L., Xu, Y., Zhang, L. and Yin, X., Effect of coating defects on oxidation behaviour of three dimensional C/SiC composites from room temperature to 1500 °C. *J. Mater. Sci.*, 2002, **37**, 5339–5344.
20. Xu, Y., Cheng, L., Zhang, L., Ying, H. and Zhou, W., Oxidation behavior and mechanical properties of C/SiC composites with Si–MoSi<sub>2</sub> oxidation protection coating. *J. Mater. Sci.*, 1999, **34**, 6009–6014.
21. Piquero, T., Vincent, H., Vincent, C. and Bouix, J., Influence of carbide coatings on the oxidation behaviour of carbon fibers. *Carbon*, 1995, **33**, 455–467.
22. Webster, J. D., Westwood, M. E., Hayes, F. H., Day, R. J., Taylor, R., Duran, A. et al., Oxidation protection coatings for C/SiC based on yttrium silicate. *J. Eur. Ceram. Soc.*, 1998, **18**, 2345–2350.
23. Zhang, Y.-L., Li, H.-J., Fu, Q.-G., Li, K. Z., Hou, D.-S. and Fei, J., A Si–Mo oxidation protective coating for C/SiC coated carbon/carbon composites. *Carbon*, 2007, **45**, 1105–1136.
24. Zhang, Y.-L., Li, H.-J., Fu, Q.-G., Li, K. Z., Wei, J. and Wang, P.-Y., A C/SiC gradient oxidation protective coating for carbon/carbon composites. *Surf. Coat. Technol.*, 2006, **201**, 3491–3495.
25. Van Wie, D. M., Drewry Jr., D. G., King, D. E. and Hudson, C. M., The hypersonic environment: required operating conditions and design challenges. *J. Mater. Sci.*, 2004, **39**, 5915–5924.
26. Henline, W. D., Thermal protection analysis of Mars–Earth return vehicles. *J. Spacecraft Rockets*, 1992, **29**, 198–207.
27. Williams, S. D., Curry, D. M., Bouslog, S. A. and Rochelle, W. C., Thermal protection system design studies for lunar crew module. *J. Spacecraft Rockets*, 1995, **32**, 198–207.
28. Steinacher, A., Lange, H., Weiland, S. and Hudrisier, S., Development of CMC body flaps for future re-entry vehicles. In *Proceedings of the 58th International Astronautical Congress*, 2007.
29. Hald, H. and Winkelmann, P., TPS development by ground and reentry flight testing of CMC materials and structures. In *Proceedings of 2nd European Workshop on Thermal Protection Systems (ESA)*, 1995.
30. Hald, H. and Winkelmann, P., Post mission analysis of the heat shield experiment CETEX for the EXPRESS capsule. In *Proceedings of the 48th International Astronautical Congress. International Astronautical Federation*, 1997.
31. Brix, P. and Herzberg, G., The dissociation energy of oxygen. *J. Chem. Phys.*, 1953, **21**, 2240.
32. Brook, M. and Kaplan, J., Dissociation energy of NO and N<sub>2</sub>. *Phys. Rev.*, 1954, **96**, 1540–1542.
33. Scott, C. D., Catalytic recombination of oxygen and nitrogen in high temperature reusable surface insulation. In *Progress in Astronautics and Aeronautics: Aerothermodynamics and Planetary Entry*, ed. A. L. Crosbie. AIAA, New York, 1981, pp. 192–212.
34. Rakich, J. V., Stewart, D. A. and Lanfranco, M. J., Results of a flight experiment on the catalytic efficiency of the Space Shuttle heat shield. AIAA Paper 82-0944, June 1982.
35. Stewart, D. A., Rakich, J. V. and Lanfranco, M. J., Catalytic surface effects on space shuttle thermal protection system during earth entry of flights STS-2 through STS-5. NASA CP-2283, Part 2, 1983, p. 827.
36. Scott, C. D., Effects of nonequilibrium and wall catalysis on shuttle heat transfer. *J. Spacecraft Rockets*, 1985, **41**, 489–499.
37. Marschall, J., Chamberlain, A., Crunkleton, D. and Rogers, B., Catalytic atom recombination on ZrB<sub>2</sub>/SiC and HfB<sub>2</sub>/SiC ultrahigh-temperature ceramic composites. *J. Spacecraft Rockets*, 2004, **41**, 576–581.
38. Dogigli, M., Pradier, A. and Tumino, G., Advanced key technologies for hot control surfaces in space re-entry vehicles. In *Proceedings of the 34th COSPAR Scientific Assembly*, 2002.
39. Dogigli, M., Pfeiffer, H., Eckert, A. and Fröhlich, A., Qualification of CMC body flaps for X-38. In *Proceedings of the 52nd International Aeronautical Congress*, 2001.
40. Mühlratzer, A., Köberle, H., Peetz, K. and Wildenrotter, K., Design and manufacture of CMC materials for reentry vehicles. In *Proceedings of the 3rd European Workshop on TPS*, 1998.
41. Balat-Pichelin, M., Robert, J. F. and Sans, J. L., Emissivity measurements on carbon–carbon composites at high temperature under high vacuum. *Appl. Surf. Sci.*, 2006, **253**, 778–783.
42. Balat-Pichelin, M., Hernandez, D., Olalde, G., Rivoire, B. and Robert, J. F., Concentrated solar energy as a diagnostic tool to study materials under extreme conditions. *J. Sol. Energy Trans. ASME*, 2002, **124**, 215–222.
43. Paulmier, T., Balat-Pichelin, M., Le Quéau, D., Berjoan, R. and Robert, J. F., Physico-chemical behaviour of carbon materials under high temperature and ion irradiation. *Appl. Surf. Sci.*, 2001, **180**, 227–245.
44. Paulmier, T., Balat-Pichelin, M. and Le Quéau, D., Structural modifications of carbon–carbon composites under high temperature and ion irradiation. *Appl. Surf. Sci.*, 2005, **243**, 376–393.
45. Dunlap Jr., P. H., Steinetz, B. M., Curry, D. M. and DeMange, J. J., Investigations of a control surface seal for reentry vehicle. *J. Spacecraft Rockets*, 2003, **40**, 570–583.
46. Cleland, J. and Iannetti, F., Thermal protection system of the space shuttle. NASA CR-4227, N89-26046, 1989.
47. Balat-Pichelin, M., Badie, J. M., Berjoan, R. and Boubert, P., Recombination coefficient of atomic oxygen on ceramic materials under earth re-entry conditions by optical emission spectroscopy. *Chem. Phys.*, 2003, **291**, 181–194.
48. Balat-Pichelin, M., Bedra, L., Gerasimova, O. and Boubert, P., Recombination of atomic oxygen on  $\alpha$ -Al<sub>2</sub>O<sub>3</sub> at high temperature under air microwave-induced plasma. *Chem. Phys.*, 2007, **340**, 217–226.
49. Balat, M., Czerniak, M. and Badie, J. M., Thermal and chemical approaches for oxygen catalytic recombination evaluation on ceramic materials at high temperature. *Appl. Surf. Sci.*, 1997, **120**, 225–238.
50. Balat-Pichelin, M. and Vesel, A., Neutral oxygen atom density in the MESOX air plasma solar furnace facility. *Chem. Phys.*, 2006, **327**, 112–118.
51. Scatteia, L., Borrelli, R., Cosentino, G., Bechê, E., Sans, J.-L. and Balat-Pichelin, M., Catalytic and radiative behaviors of ZrB<sub>2</sub>–SiC ultrahigh temperature ceramic composites. *J. Spacecraft Rockets*, 2006, **43**, 1004–1012.
52. Scatteia, L., Alfano, D., Monteverde, F., Sans, J.-L. and Balat-Pichelin, M., Effect of machining method on catalytic and emissivity of ZrB<sub>2</sub> and ZrB<sub>2</sub>–HfB<sub>2</sub>-based ceramics. *J. Am. Ceram. Soc.*, 2008, **91**, 1461–1468.
53. Arrhenius, S., Über die Reaktionsgeschwindigkeit bei der Inversion von Rohrzucker durch Sauren. *Z. Phys. Chem.*, 1889, **4**, 226.